

LA-UR- 08-7023

Approved for public release;
distribution is unlimited.

Title: Age Characteristics in a Multidecadal Arctic Sea Ice Simulation

Author(s): Elizabeth Hunke, 108213, T-3

Intended for: Journal of Geophysical Research--Oceans



Los Alamos National Laboratory, an affirmative action/equal opportunity employer, is operated by the Los Alamos National Security, LLC for the National Nuclear Security Administration of the U.S. Department of Energy under contract DE-AC52-06NA25396. By acceptance of this article, the publisher recognizes that the U.S. Government retains a nonexclusive, royalty-free license to publish or reproduce the published form of this contribution, or to allow others to do so, for U.S. Government purposes. Los Alamos National Laboratory requests that the publisher identify this article as work performed under the auspices of the U.S. Department of Energy. Los Alamos National Laboratory strongly supports academic freedom and a researcher's right to publish; as an institution, however, the Laboratory does not endorse the viewpoint of a publication or guarantee its technical correctness.

1 **Age Characteristics in a Multidecadal Arctic Sea Ice**
2 **Simulation**

Elizabeth C. Hunke

3 Fluid Dynamics Group, Theoretical Division, Los Alamos National
4 Laboratory, Los Alamos, New Mexico, USA

Cecilia M. Bitz

5 Atmospheric Sciences, University of Washington, Seattle, Washington, USA

E. C. Hunke, MS-B216 Los Alamos National Laboratory, Los Alamos, NM 87545, USA.
(eclare@lanl.gov)

C. M. Bitz, Atmospheric Sciences box 351640, University of Washington, Seattle WA 98195-
1640 USA. (bitz@atmos.washington.edu)



6 **Abstract.** Results from adding a tracer for age of sea ice to a sophisti-
7 cated sea ice model that is widely used for climate studies are presented. The
8 consistent simulation of ice age, dynamics, and thermodynamics in the model
9 shows explicitly that the loss of perennial ice accelerated in the past three
10 decades, as has been seen in satellite-derived observations. Our model shows
11 that the September ice age average across the Northern Hemisphere varies
12 from about five to eight years and the ice is much younger (about two to three
13 years) in late winter due to the expansion of first-year ice. We find seasonal
14 ice on average comprises about 5% of the total ice area in September, but
15 as much as $1.36 \times 10^1 \text{ km}^1$ survives in some years. Our simulated ice age in
16 the late 1980s and early 1990s declined markedly in agreement with other
17 studies. However, after this period of decline, the ice age began to recover.
18 As a result we find little trend in the average ice age over the last three decades.
19 In contrast, ice area, thickness and volume declined over the same period,
20 particularly for perennial ice, with an apparent acceleration in the last decade.



1. Introduction

21 The sea ice cover in the Northern Hemisphere is undergoing significant changes, the
22 most threatening being a shift from a mostly perennial pack to an ice cover dominated by
23 seasonal ice, as in the Antarctic [*Rigor and Wallace, 2004; Maslanik et al., 2007*]. This
24 is of fundamental concern for native peoples and wildlife that depend on the pack ice for
25 their livelihoods. We do not yet know the magnitude of potential future climate change
26 that could be associated with such a shift in the Arctic, but climate models indicate that
27 sea ice related feedbacks contribute to polar amplification of the global warming signal
28 [e.g., *Holland and Bitz, 2003*].

29 Beginning in the late 1970s, the satellite era opened a viewing window for the large-scale
30 variability of the polar regions. While the satellite record is limited in length and consists
31 primarily of sea ice area concentration deduced from brightness temperatures [*Gloersen*
32 *et al., 1992*], substantive changes to the Arctic sea ice pack over the past decade are be-
33 coming apparent nevertheless, particularly as reductions in area coverage in summer [e.g.,
34 *Comiso et al., 2008*]. Although more difficult to observe, other fundamental character-
35 istics of the pack ice are also changing, such as ice thickness [*Wadhams, 1990; Rothrock*
36 *et al., 1999; Wadhams and Davis, 2000*]. Several factors influence whether ice survives
37 the melt season, including thickness [*Bitz and Roe, 2004*], variations in atmospheric and
38 oceanic temperature and circulation patterns [*Comiso et al., 2003*], and the duration of
39 the melt season [*Belchansky et al., 2004*].

40 Efforts to infer or measure other variables from satellites, such as sea ice thickness
41 and velocity, is progressing [e.g., *Laxon et al., 2003; Kwok et al., 2004a*], and synthesis



of technologies enable derivation of additional quantities. In light of research suggesting recent thinning of Arctic sea ice [e.g., *Rothrock et al.*, 1999], and in the absence of basin-wide, detailed thickness observations, there has been much interest in obtaining ice age estimates from satellite data, with which to infer and understand changes in the volume of Arctic sea ice. Ice thickness is closely related to the age of the ice, because thickening through dynamic processes such as ridging accumulates over time. *Johannessen et al.* [1999] initiated the effort using satellite passive microwave data for November through March, 1978–1998. Surface emissivities of open water, first-year and multi-year (perennial) ice are sensitive to the sensor frequency and if they are assumed to be relatively stable in winter, ice age can be crudely distinguished. *Johannessen et al.* related trends in perennial ice area to thickness changes inferred from surface elastic-gravity wave measurements.

However, the stability assumptions of their method are questionable [*Comiso*, 2002; *Fowler et al.*, 2004]; *Comiso* [2002] simply defined multi-year ice to be that ice remaining at the end of the summer melt season in September, determined from a 7-day running mean of satellite-derived minimum ice extent for 1978–2000. In a different approach, *Rigor and Wallace* [2004] fed monthly gridded ice motion fields from Arctic buoys [*Rigor et al.*, 2002] and September ice concentration data into to a simple advection model, tracking the ice until the following September. Ice remaining within the 90% ice concentration contour was aged one year. Using this procedure, they obtained ice age estimates for the last several decades, through 2002. *Fowler et al.* [2004] employed a similar technique, but using daily Advanced Very High Resolution Radiometer (AVHRR) ice velocities, averaged to weekly, and a 40% ice concentration threshold. *Belchansky et al.* [2005] also used an ice-tracking approach, but backwards in time, generating ice age maps for 1989–2003 by



65 aging pixels within the 15% concentration contour each month, until reaching the time
66 and location of the ice's origin. *Nghiem et al.* [2007] returned to the ideas of *Johannessen*
67 *et al.* [1999], exploiting distinctive backscatter signatures from the QuikSCAT satellite to
68 identify seasonal, perennial, and a "mixed" ice class. Finally, *Maslanik et al.* [2007] used
69 the *Fowler et al.* [2004] approach, coupled with ICESat laser altimeter ice thickness data
70 for 2003–2006, to develop an ice thickness proxy that could be used to create maps of ice
71 volume in prior years via thickness correlations with satellite-based ice age.

72 The overall results from these various methods are similar, although they differ in the
73 details. All indicate a reduction of older ice types in the Arctic over the past several
74 decades, in general agreement with observations of a thinning ice pack. The eastern
75 Arctic Ocean is dominated by younger ice, while older ice resides in the western Arctic, in
76 and near the Canadian Archipelago. Perennial ice classes are recruited from first-year ice
77 formed primarily in the eastern Arctic and north of Alaska. Some of this ice is entrained
78 into the Beaufort Gyre where it recirculates, ridging and thickening until it is ejected into
79 the Transpolar Drift Stream, which carries ice across the North Pole and out of the Arctic
80 through Fram Strait. Northward retreat of the summer ice edge from the North American
81 coast has cut short the recirculation of ice in the Beaufort Gyre, leaving thinner ice that
82 melts more easily in the gyre [*Rigor and Wallace*, 2004; *Belchansky et al.*, 2005; *Maslanik*
83 *et al.*, 2007].

84 Older ice, and by association thicker ice, possesses different characteristics than younger,
85 thinner ice by virtue of the aging process, particularly desalination through brine channels
86 and associated changes in albedo [*Perovich*, 2003]. Changes in the physical characteristics



of the ice pack due to its transition from older to younger ice will have ramifications for the strength of feedbacks [Perovich *et al.*, 2008] and ecosystem structure [Lizotte, 2001].

No studies of sea ice age to date have used a full-physics sea ice model with a consistent method for determining age and thickness. Here we present a 59-year Arctic simulation with a new implementation of the Los Alamos sea ice model, CICE version 4.0, which includes a representation of sea ice age.

2. Model description

The sea ice model employed here, CICE version 4.0, features many software and physics enhancements over previous versions. The model infrastructure was thoroughly overhauled for improved performance and flexibility, including a straight-forward mechanism for adding tracers such as ice age, melt ponds, and biological or chemical compounds that are carried on (or in) the ice and snow. A tracer already found in a few sea ice models (e.g., previous versions of CICE) is surface temperature, which evolves thermodynamically and is transported with the ice as

$$\frac{\partial (i_n \theta_n)}{\partial t} + \nabla \cdot (i_n \theta_n \mathbf{u}) = 0 \quad (1)$$

where i_n is the ice area fraction of thickness category n , θ_n is the tracer quantity in category n , \mathbf{u} is ice velocity and t represents time. Transport of other tracers may be volume weighted, in which case the transport equation takes the form

$$\frac{\partial (v_n \theta_n)}{\partial t} + \nabla \cdot (v_n \theta_n \mathbf{u}) = 0 \quad (2)$$

Transport of snow volume tracers would use the snow volume, v_{sn} , instead of the ice volume, v_{in} . In CICE, ice age is an ice volume tracer following equation (2).



95 In CICE, modeled ice and snow volumes fluctuate due to thermodynamic growth and
96 melt following *Bitz and Lipscomb* [1999], horizontal transport via incremental remapping
97 [*Lipscomb and Hunke*, 2004], and mechanical redistribution (that is, rafting and ridging),
98 based on *Thorndike et al.* [1975], *Rothrock* [1975], *Hibler* [1980], *Flato and Hibler* [1995],
99 *Bitz et al.* [2001] and *Lipscomb et al.* [2007]. Ice is transferred among thickness cate-
100 gories using the remapping scheme of *Lipscomb* [2001]. We use the elastic-viscous-plastic
101 (EVP) ice dynamics model of *Hunke and Dukowicz* [2002], as modified by *Connolley et al.*
102 [2004], to find the ice velocity. Velocity components are used for horizontal ice transport,
103 and spatial derivatives of velocity (ice deformation or strain rates) drive the mechanical
104 redistribution.

105 The incremental remapping scheme is conservative, non-oscillatory, second-order accu-
106 rate in space, and monotonicity-preserving for tracers; that is, it does not create new
107 extrema. The accuracy may be reduced locally to first order to preserve monotonicity.
108 The characteristic that sets incremental remapping apart from other advection schemes is
109 that it is efficient for large numbers of thickness categories or tracers. Much of the work
110 needed to remap spatial quantities from one time step to the next is geometrical and per-
111 formed once per grid cell. Additional categories or tracers utilize the existing geometrical
112 information, requiring only a small amount of extra work [*Lipscomb and Hunke*, 2004].

113 In the configuration used here, CICE partitions the ice pack in each grid cell into a
114 5-category ice thickness distribution, with 4 ice layers and 1 snow layer in each category.
115 State variables for each thickness category include ice area and surface temperature, plus
116 ice or snow volume and enthalpy for each layer within each thickness category. (The
117 thickness category ranges are 0–0.64 m, 0.64–1.39 m, 1.39–2.47 m, 2.47–4.57 m, and



118 greater than 4.57 m.) Because ice volume is the product of area and thickness, $V_{in} = A_{in} h_{in}$,
119 ice thickness can be considered an ice area tracer (Eq. 1). Similarly, enthalpy is an ice
120 volume tracer. Counting all of these tracers, plus ice age, in all categories and layers,
121 CICE carries 45 tracer fields in addition to ice area. Although all state variables and
122 tracers are defined and modeled for each thickness category, for output and analysis the
123 category values are merged into a single value for each grid cell using the category ice
124 concentrations (or volumes, for volume tracers). Age “classes” or “types” referred to in
125 this paper are defined during the post-processing stage and used to collect ice of similar
126 ages for analysis.

127 Tracers may or may not affect the physical evolution of the pack. Although physical
128 characteristics of the ice are known to change as the ice ages (salinity reduction via brine
129 drainage, for instance), these changes are directly related to physical conditions, and we
130 therefore treat ice age as a passive tracer. Initialized at age 0 upon freezing open water
131 (e.g., frazil production), ice ages the length of the time step at each step. Melting does
132 not affect the age. In our control run, basal freezing also does not alter the age, but
133 we present results from a sensitivity run in which basal freezing makes the ice column
134 younger. Mechanical redistribution processes and advection alter the age of ice in any
135 given grid cell in a conservative manner following changes in ice volume.

136 The model is configured for the global 320×384 (1°), displaced-pole grid used for the
137 ocean and ice components of the fully-coupled Community Climate System Model version
138 3 (CCSM3) [Kiehl and Gent, 2004; Collins *et al.*, 2006], using a one-hour time step. The
139 grid spacing ranges between 20 and 85 km, averaging 40 km north of 70 N. Output from
140 the CCSM ocean component (POP) in a fully-coupled CCSM run is used for the lower



141 boundary conditions in CICE, including sea surface temperature, salinity and a deep
142 ocean heat flux. Ocean currents are set to zero. The sea surface temperature is computed
143 using a thermodynamic ocean mixed layer parameterization within CICE, which depends
144 on prescribed atmospheric forcing and the sea ice evolution.

145 Atmospheric forcing data includes 6-hourly air temperature, specific humidity, and wind
146 velocity components from the Common Ocean Reference Experiments (CORE) version 2
147 [1958-2006, *Large and Yeager*, 2008] along with monthly “normal year” precipitation from
148 version 1 [*Large and Yeager*, 2004], as described in *Hunke and Holland* [2007]. Rather than
149 reading data for shortwave and longwave radiation, we use version 2 of the Ocean Model
150 Intercomparison Project’s cloud climatology [OMIP, *Röske*, 2001] along with temperature
151 and humidity data to compute these fields following the Arctic Ocean Model Intercompar-
152 ison protocol [*Hunke and Holland*, 2007]. A stability-based atmospheric boundary layer
153 formulation is used to compute the turbulent sensible and latent heat fluxes and wind
154 stress components. The sea ice albedo follows the dual-band, thickness- and temperature-
155 dependent formulation of CCSM3. Further information regarding CICE can be found in
156 *Hunke and Lipscomb* [2008].

157 The ice state is initialized from an earlier run, as described in *Hunke and Holland* [2007].
158 Although fast ice in a few grid cells in the Canadian Arctic reaches ages concomitant with
159 the length of the run, which starts in 1958, most of the pack achieves its oldest values by
160 the mid-1970s, and we analyze the last 30 years of output.

3. Results

161 First, we clarify a point of semantics. In the nomenclature used by the World Me-
162 teorological Organization [*WMO*, 1989], *first-year ice* is “sea ice of not more than one



163 winter's growth, developing from young ice; thickness 30 cm–2 m." Thus, young ice less
164 than 30 cm thick is not classified as first-year ice. *Old ice* is "sea ice which has survived at
165 least one summer's melt . . . May be divided into *second-year* and *multi-year* ice." Second-
166 year ice has survived only one summer's melt, while multi-year ice has survived at least
167 two summers' melt. At the end of summer, ice which grew late in the preceding winter
168 and is less than one year old is reclassified as second-year ice. This nomenclature is quite
169 sensible for field observations but leads to confusion when comparing with a numerical
170 age tracer such as ours. In the spirit of the WMO nomenclature, *Belchansky et al.* [2005]
171 classify 0–4-month-old ice as "first-year," 5–15-month-old ice as "second-year," and so on.
172 Other studies include second-year ice (as defined by the WMO) in their multi-year ice
173 class [*Johannessen et al.*, 1999; *Comiso*, 2002; *Maslanik et al.*, 2007]. Following the lead
174 of *Nghiem et al.* [2007], we refer to ice which is less than 1 year old as "seasonal" ice and
175 ice older than 1 year as "perennial" ice, otherwise following the WMO nomenclature or
176 that used by the cited authors, in context.

3.1. Seasonal and perennial ice

177 We begin with an inspection of Northern Hemisphere total ice volume and area coverage,
178 broken down into seasonal and perennial ice types. Of these, the most easily compared
179 with observations is total ice area, shown in Figure 1a. The maximum and minimum
180 values compare well with satellite passive microwave data for 1978–1987 [13.9×10^7 km²
181 and 4.7×10^7 km², respectively, *Gloersen et al.*, 1992]. The ice edge, especially in winter,
182 is strongly controlled by the amount of heat available from the ocean [*Bitz et al.*, 2005],
183 and because ice area concentration is nearly 100% in winter, the same is true for total
184 winter ice area. Here, ocean heat flux from a CCSM simulation is input as an annually



185 repeating monthly-mean climatology and hence the resulting area simulation varies little
186 from year to year at its winter maximum. Interannual atmospheric variability becomes
187 more prevalent in warmer months when albedo feedbacks intensify and the ice edge retreats
188 from regions with strong ocean heat flux convergence.

189 In contrast, the area covered by perennial ice fluctuates from year to year even in winter,
190 as indicated in Figure 1b, and represents a significant influence on the total volume of
191 perennial ice.

192 Winter variability of seasonal ice area in this simulation (Figure 1c) is the difference
193 between the total ice area and the perennial ice area, and hence it also is constrained by the
194 prescribed oceanic heat flux. In summer, seasonal ice occasionally disappears altogether,
195 but up to $1.86 \times 10^1 \text{ km}^1$ survives to become perennial ice in some years (Fig. 1d).
196 By September, on average only 5% of the total ice area is seasonal ice. However, the
197 September total ice area anomaly, also shown in Fig. 1d, is correlated with the September
198 seasonal ice area with a correlation coefficient of 0.54 when linear trends are removed (the
199 correlation is for the period 1977–2006 and is significant at the 95% confidence level).

200 Although the total volume of seasonal ice is somewhat limited by the length of time
201 during which it can grow, so that it remains relatively thin compared with older ice,
202 it nevertheless contributes significantly to the seasonal cycle of total ice volume; the
203 amplitude of the seasonal perennial ice volume cycle is about $6 \times 10^1 \text{ km}^1$ (Figure 1b),
204 while the total volume cycle is roughly $13 \times 10^1 \text{ km}^1$ (Figure 1a), the remainder being
205 made up of $\sim 7 \times 10^1 \text{ km}^1$ of $\sim 1\text{-m}$ young ice.

206 Transport of ice through Fram Strait into the North Atlantic, where it melts, is known
207 to be a significant factor in the loss of Arctic perennial ice types [*Rigor and Wallace, 2004*;



208 *Nghiem et al.*, 2007]. The model simulates this transport well, as compared with satellite-
209 based observational data [*Kwok et al.*, 2004a] (Figure 2), although the variability of fluxes
210 is larger in the simulation than in the observations. The flux gate used for analysis of
211 the satellite data is in a slightly difference place than the grid line used for the model
212 calculation; the endpoints of the flux gate for the model estimates are (79.9N, 16W) and
213 (80.3N, 20E).

214 Figure 1e shows the Northern-Hemisphere-average sea ice age for perennial and all ice
215 classes. Perennial ice reaches a quasi-equilibrium age by the mid-1970s. The maximum
216 value during each year occurs at the end of summer, when perennial ice area is as its min-
217 imum. In the early 1980s the area covered by younger ice shrank, causing the maximum
218 in ice age seen here in 1981. This is associated with the extended period of high ice flux
219 through Fram Strait (Figure 2) and will be discussed in more detail later.

220 The mean annual cycle of perennial ice volume, area, thickness and age for three decades
221 beginning in 1977 is shown in Figure 3. The simulation indicates that loss of perennial ice
222 volume has accelerated, in agreement with satellite-derived observations [*Comiso*, 2006;
223 *Nghiem et al.*, 2007; *Comiso et al.*, 2008], primarily due to decreasing ice thickness. In-
224 terestingly, the average ice age had little trend in the past 2 decades, following a 1-year
225 shift to younger ice after 1981.

226 Statistics for the full 1977–2006 period, given in Table , highlight the trend of seasonal
227 ice partially replacing perennial ice in March, with a net decrease in area overall and a
228 concomitant reduction in average age. Both ice types are declining in September.



3.2. Sea ice thickness and age

229 *Maslanik et al.* [2007] used ice age and ice thickness from March satellite observations
230 during 2003–2006 (described in more detail in the Introduction) to obtain a proxy data
231 set of ice thickness, assuming that older ice is thicker than younger ice. Their results are
232 shown in Figure 4 against the output from our model simulation. Agreement is remarkably
233 good for ice up to 10 years old. Five- to eight-year-old ice was slightly thicker in earlier
234 decades. Ice beyond 10 years of age continues to age but at a hemispherically averaged
235 rate slower than actual time. For instance, by the end of the second decade illustrated
236 here, the simulation has run for 39 years, but there is no ice older than 26 years in the
237 hemispheric average. This discrepancy is due to the incorporation of first-year lead ice
238 within the pack and from the marginal ice zone.

239 Neither spatial patterns nor interannual variability of ice age and ice thickness are as
240 closely related as might be deduced from the *Maslanik et al.* [2007] proxy. Figure 5
241 illustrates modeled ice thickness and age in March of 1976, 1986, 1996 and 2006. Near the
242 Canadian Archipelago, where ice is very thick and old, and near the Siberian coast, where
243 ice tends to be thin and young, the age and thickness contours line up well. In the central
244 Arctic, however, dynamic processes contribute to the complexity of the pack’s physical
245 characteristics through large-scale ice motion (Beaufort Gyre, transpolar drift and export
246 through Fram Strait) and smaller scale processes such as rafting and ridging.

247 In our simulation, the oldest ice is consistently located in the Canadian Arctic where the
248 pack is thick and relatively stationary. Looking only at the central Arctic Ocean region
249 (i.e., excluding the Canadian Arctic), we see that the Beaufort Gyre holds the oldest ice in
250 1976, which continues to age as it recirculates [*Rigor and Wallace, 2004*]. By 1986 a band



251 of older ice reaches across the southern Arctic Ocean from northern Greenland west to
252 eastern Siberia, encircling a bight of younger ice. This pattern reflects both the Beaufort
253 Gyre's circulation pattern and the Transpolar Drift's large export of ice through Fram
254 Strait a few years earlier. In 1996 older (and thicker) ice is compressed along the Canadian
255 Archipelago, with indications of transport around the southern flank of the Beaufort Gyre.
256 By 2006 the central Arctic has refilled with older ice, although it is neither as old nor as
257 thick as that seen in previous decades.

258 Interannual variability of ice age does not have a strong positive correlation with ice
259 thickness, volume, or extent when averaged north of 70N or for the whole Northern Hemi-
260 sphere (see Figure 1). The strongest relation we found was in fact a *negative correlation*
261 between September ice age and September area ($r = -0.68$, significant at greater than
262 95% confidence level). The negative correlation derives from the fact that anomalously
263 low seasonal ice coverage leaves a proportionately above-average amount of perennial ice
264 behind, which causes the ice that remains to be older than average while at the same time
265 giving rise to anomalously low ice area.

3.3. Processes affecting sea ice age

266 Ice volume at any given point in time represents a time-integrated history of the many
267 processes acting on sea ice. Similarly, ice age reflects both calamity and serenity during the
268 unrelenting march of time. Figure 6a illustrates these contrasts in the form of a Hovmüller
269 diagram. The area coverage of one- to six-year-old ice is fairly constant from the mid-
270 1970s through 1990, indicating fairly consistent conversion from younger ice types. The
271 1981 maximum in ice age seen in Figure 1e is evident here as a moderate reduction in the
272 area of roughly two- to six-year-old ice beginning in 1980, while older ice types maintain



273 their coverage. During the 1990s, however, larger areas of younger ice are present while
274 ice classes older than 6 years fail to be repopulated. The younger ice types gradually
275 age until six-year and older ice is replenished in the mid-2000s. Meanwhile during the
276 last decade of the run, area coverage by the youngest ice types diminishes, leading to the
277 relatively old maxima in average ice age seen at the end of the run (Figure 1e).

278 Figure 6b illustrates these changes in a slightly different way, as the cumulative area of
279 ice older than a given age. The cumulative presentation emphasizes the transient features,
280 making it easier to see a temporary reduction in two- to six-year-old ice in the early 1980s.
281 The mid-1990s show a unique reduction in six-year and older ice after the prolonged loss
282 of younger ice that would normally replenish the older ice classes. As a result, the basin-
283 wide average age reaches a minimum in 1997. Our results agree with *Belchansky et al.*
284 [2005], who observed that considerable areas of first-year ice survived the melt season in
285 the mid-1990s (see spikes in the 1992 and 1996 in our Figure 1d), which then rebuild
286 multi-year ice area in the late 1990s. However our results also show that the repopulation
287 of multi-year ice classes was only temporary since younger ice types again declined in the
288 2000s, lending uncertainty to the future of the ice pack.

289 Our results also broadly agree with those of *Rigor and Wallace* [2004], who use an
290 advection model with observational input data. However, our ice tends to be younger
291 than theirs in the 1980s because deformation in our model ridges and rafts younger,
292 thinner ice, effectively lowering the age of older, thicker ice. By the end of summer in the
293 1980s, most of the Arctic in Rigor and Wallace's study was covered by ice older than 10
294 years; in contrast our Northern-Hemisphere-average ice is generally about 7 years old at
295 the end of summer in the 1980s. By September 2002, most of the ice age in Rigor and



296 Wallace's study is less than 5 years old, at the same time our model ice age still averages
297 between 6 and 7 years. Furthermore, our model clearly indicates that the declining trend
298 in ice area and thickness is not commensurate with consistent loss of ice of any particular
299 age, nor a decline in average ice age overall.

300 We find it more difficult to compare with the studies of *Maslanik et al.* [2007] and
301 *Fowler et al.* [2004] because their figures combine all ice greater than 5 years of age in one
302 bin. They discuss ice age differences between years with apparent extrema, rather than
303 trends; the range of our extrema are similar to theirs. Their ice age appears to show some
304 recovery in the early 2000s, as does ours and that of *Belchansky et al.* [2005].

305 Dynamical processes act to decrease the volume of older ice in two ways: first by
306 incorporating younger ice into the old through advection and mechanical deformation,
307 and second by transporting ice to the marginal ice zone where it melts. In our simulation,
308 the transport of ice through Fram Strait (Figure 2) is a strong dynamical influence on the
309 age characteristics of the Arctic sea ice pack. Two- to six-year-old ice comprises much of
310 the Fram Strait ice export, which all melts eventually. The extended period of high flux
311 rates in the early 1980s carried much young ice out of the Arctic (Figure 6c), depleting
312 these age classes and resulting in the flux of 6-year and older ice through Fram Strait
313 in subsequent years. 1986 saw another period of young ice export, but rates were low
314 (Figure 2). In the late 1980s flux rates again increased, this time carrying much older
315 ice. This resulted in the depletion of older ice types seen in the early 1990s [*Rigor and*
316 *Wallace, 2004*].

317 *Kwok and Rothrock* [1999] and *Rigor et al.* [2002] examine the correlation of ice fluxes
318 through Fram Strait with the North Atlantic and Arctic Oscillation (AO) indices. Briefly,



319 high AO signals in winter are associated with increased advection of ice away from the
320 Eurasian coast and through Fram Strait, while low AO conditions lead to more open
321 water in the Beaufort and Chukchi Seas and increased circulation of the Beaufort Gyre,
322 which carries more ice to the marginal ice zone north of Alaska [*Rigor and Wallace,*
323 2004]. The AO was substantially higher than normal from late 1988 through 1994 and
324 more neutral since 1995, except for a moderately high period in 2000–2002 and again in
325 2007. Our results suggest that the ice age began to recover in 1995, despite the fact that
326 the declining trend in ice area and thickness continued. These results suggest that the
327 AO has a large influence on ice age, but the decline in actual area and thickness is more a
328 function of the increase in greenhouse warming. This suggestion is supported by the fact
329 that in 20th and 21st century projections by global climate models, ice area and thickness
330 tend to decline considerably [e.g., *Arzel et al., 2006; Zhang and Walsh, 2006*] with little
331 or no trend in the AO [*Gillett et al., 2002*].

332 A typical indicator of basin-wide thermodynamic effects is melt season length, or dates
333 of melt or freeze onset. Using satellite passive microwave measurements of brightness
334 temperature in conjunction with National Center for Environmental Prediction (NCEP)
335 reanalysis surface air temperatures for 1979–1996, *Smith [1998]* found an increase in melt
336 season length of 4.5 days per decade for perennial ice within the Arctic Ocean. Using
337 an updated algorithm, *Belchansky et al. [2004]* estimated the analogous change in melt
338 season length at 5.5 days per decade. We compute a similar positive trend of 6.7 days
339 per decade for the full Northern Hemisphere (Table 1). Differences in melt season length
340 stem from differences in the analyzed area (Arctic Ocean versus Northern Hemisphere)
341 and algorithms for identifying perennial ice as well as the method for identifying melt and



342 freeze onset dates. Seasonal ice was not experiencing as drastic a change as perennial ice;
343 our modeled trend in melt duration for all Northern Hemisphere ice is an increase of 4.7
344 days per decade for 1979–1996. For the 1979–2006 period, however, the melt duration for
345 seasonal and perennial ice types both increased 6.5 days per decade.

3.4. Ice column age

346 In the simulation described above, the addition of new ice on the bottom of existing ice
347 did not affect the age of the ice in that thickness category, so that our results would be
348 more comparable to those derived from satellite observations. To find out how sensitive
349 the sea ice age is to vertical thermodynamic accretion, we performed a second simulation
350 identical to the first except that the volume of new bottom ice is given an initial age equal
351 to the timestep ($\Delta t = 1$ hr) which is then volume-averaged with the age of the existing
352 ice. Spatial patterns in the resulting age maps are similar to the control run results, but
353 the ice is much younger overall, as is evident in Figure 7, highlighting the prominent role
354 that seasonal ice already plays in the Arctic. Not only is it a significant—and growing—
355 fraction of the total area covered by sea ice on a seasonal basis, new ice at the bottom of
356 the ice column reduces the average “true” age of the pack and contributes its own physical
357 properties to the ice column.

358 Some of the ice accreted onto the bottom of the pack melts, resulting in a loss of
359 relatively young ice from the ice column. In this simulation we do not track the age of ice
360 layers within the ice column, only the average age of the ice thickness category, and are
361 thus unable to adjust the age appropriately upon melting. Therefore this sensitivity test
362 represents a lower bound for the age of the ice pack.



4. Conclusions

363 Sparsity of high latitude, *in situ* observational data has led researchers to clever uses
364 of satellite and ground-based measurements. Total ice volume remains just out of reach,
365 although thickness estimates are becoming available [e.g., *Kwok et al.*, 2004b]. As remote
366 sensing technology progresses, combinations of techniques may enable us to reconstruct
367 the history of the polar ice cover, as *Maslanik et al.* [2007] demonstrate with their initial
368 ice thickness proxy. In the meantime, sea ice models such as CICE attempt to fill in the
369 gaps, particularly subsurface processes that satellites can not see.

370 In CICE, each thickness category in the ice-thickness distribution has a unique thick-
371 ness, ice age, concentration, snow depth, temperature profile, albedo, and set of surface
372 fluxes. Ice motion is computed by the model with a one-hour time step for the velocity
373 field, ice advection, and deformation. The model is forced with 4-hourly varying atmo-
374 spheric conditions for 1958–2006. Thus our model computes ice age in a consistent fashion
375 with evolution of ice dynamics and thermodynamics. In contrast, previous studies that
376 presented ice age in detail used observations to derive ice motion, deformation, and ex-
377 tent, with an advection and deformation time step of one month [*Rigor and Wallace*,
378 2004] or one week [*Fowler et al.*, 2004; *Maslanik et al.*, 2007]. *Rigor and Wallace* [2004]
379 use an empirical relation to estimate ice growth that is independent of snow depth and
380 atmospheric conditions. *Fowler et al.* [2004] and *Maslanik et al.* [2007] do not model ice
381 growth or melt processes, instead using satellite imagery to determine areas of ice loss or
382 new ice growth.

383 The consistent simulation of ice age, dynamics, and thermodynamics in our model
384 agrees well with the large spatial-scale, multi-year, average sea ice thickness–age relation



385 that was derived from observations by *Maslanik et al.* [2007]. Our model shows explicitly
386 the accelerating loss of perennial ice over the past three decades that has been seen in
387 satellite-derived observations [*Nghiem et al.*, 2007; *Corniso et al.*, 2008].

388 Our model also shows that the September average ice age across the Northern Hemi-
389 sphere varies from about five to eight years and the ice is much younger (about two to
390 three years) in late winter due to the expansion of first-year ice. We find first-year ice
391 on average comprises about 5% of the total ice area in September, but as much as 1.36
392 $\times 10^1$ km¹ survive in some years. Seasonal ice area in September has not declined signif-
393 icantly in recent decades, thus the declining trend in total area in September is a result
394 of the decline in perennial ice area. Nonetheless, interannual variability in the September
395 area depends significantly on anomalies in the seasonal ice area.

396 We find that ice age in the late 1980s and early 1990s declined markedly in agreement
397 with *Rigor and Wallace* [2004] for the same reason they cite, owing to anomalously high
398 flushing of older ice out through Fram Strait during high-index years of the Arctic Os-
399 cillation. However, when the AO returned to more neutral conditions, the ice age began
400 to recover. In contrast, the ice area, thickness and volume declined throughout the past
401 three decades, with an apparent acceleration in the last decade, particularly in peren-
402 nial ice volume. Younger ice classes began to decline again in the last few years of our
403 integrations.

404 Although our model exhibits the expected relationship between ice age and thickness on
405 multi-year and Northern Hemisphere-wide averages, we find that the correlation between
406 ice age and thickness breaks down at the local scale (100s of kilometers and smaller)
407 in individual years. Furthermore, on interannual timescales, the Northern Hemisphere



408 average ice age is not well correlated with ice thickness, volume, or area. In fact, the
409 September ice age is negatively correlated with September ice area, as anomalously low
410 first-year coverage causes the average age in September to increase coincident with below
411 average area. Thus our results show that ice age is not a good proxy for sea ice thickness
412 in a given year, and it is no surprise that the area and thickness of sea ice may decline,
413 while at the same time the ice age may have little trend.

414 Comparison of model output with remote sensing data is problematic partly because of
415 disparities in scale, but also because of different methods for defining physical quantities,
416 such as melt season length and ice age. Due to constant incorporation of young ice within
417 the pack, the mean age of the simulated pack (or of ice in a grid cell) is younger than
418 would be indicated by marking certain floes and aging them with each step of an advection
419 algorithm or series of satellite images. The actual age of a given column of ice may be
420 younger yet because of bottom accretion. Our ice age results are in good agreement with
421 *Rigor and Wallace* [2004] in the later years of their integration, but their ice tends to be
422 much older at the beginning of their analysis period. Thus their results show a substantial
423 reduction in ice age, while ours do not.

424 Nevertheless, our model simulation reinforces the observationalists' story: older ice
425 types have declined in the Arctic ice cover, partly through Fram Strait export. Some young
426 ice survives to repopulate the older classes, but the area covered by ice less than 5 years old
427 has shrunk considerably since 2000. In the coming decades, it is possible that the age of the
428 Arctic ice pack will fluctuate between younger and older ice types, sometimes exhibiting
429 bimodal age distributions as in the 1990s, before becoming completely dominated by
430 seasonal ice.



431 **Acknowledgments.** E. Hunke is supported by the Climate Change Prediction Pro-
432 gram of the Department of Energy's Office of Biological and Environmental Research.

References

- 433 Arzel, O., T. Fichefet, and H. Goosse (2006), Sea ice evolution over the 20th and 21st
434 centuries as simulated by the current AOGCMs, *Ocn. Mod.*, *12*, 401–415.
- 435 Belchansky, G. I., D. C. Douglas, and N. G. Platonov (2004), Duration of the Arctic sea
436 ice melt season: Regional and interannual variability 1979–2001, *J. Clim.*, *17*, 67–80.
- 437 Belchansky, G. I., D. C. Douglas, and N. G. Platonov (2005), Spatial and temporal
438 variations in the age structure of Arctic sea ice, *Geophys. Res. Lett.*, *32*, L18,504,
439 doi:10.1029/2005GL023,976.
- 440 Bitz, C. M., and W. H. Lipscomb (1999), An energy-conserving thermodynamic sea ice
441 model for climate study, *J. Geophys. Res.–Oceans*, *104*, 15,669–15,677.
- 442 Bitz, C. M., and G. H. Roe (2004), A mechanism for the high rate of sea ice thinning in
443 the Arctic Ocean, *J. Clim.*, *17*, 3623–3632.
- 444 Bitz, C. M., M. M. Holland, A. J. Weaver, and M. Eby (2001), Simulating the ice-thickness
445 distribution in a coupled climate model, *J. Geophys. Res.–Oceans*, *106*, 2441–2463.
- 446 Bitz, C. M., M. M. Holland, E. C. Hunke, and R. E. Moritz (2005), Maintenance of the
447 sea-ice edge, *J. Clim.*, *18*, 2903–2921.
- 448 Collins, W. D., C. M. Bitz, M. L. Blackmon, G. B. Bonan, C. S. Bretherton, J. A. Carton,
449 P. Chang, S. C. Doney, J. J. Hack, T. B. Henderson, J. T. Kiehl, W. G. Large, D. S.
450 McKenna, B. D. Santer, and R. D. Smith (2006), The Community Climate System
451 Model Version 3 (CCSM3), *J. Clim.*, *19*, 2122–2143.



- 452 Comiso, J. C. (2002), A rapidly declining perennial sea ice cover in the Arctic, *Geophys.*
453 *Res. Lett.*, *29*, doi:10.1029/2002GL015650.
- 454 Comiso, J. C. (2006), Abrupt decline in the Arctic winter sea ice cover, *Geophys. Res.*
455 *Lett.*, *33*, L18,504, doi:10.1029/2006GL027,341.
- 456 Comiso, J. C., J. Yang, S. Honjo, and R. A. Krishfield (2003), Detection of
457 change in the Arctic using satellite and in situ data, *J. Geophys. Res.*, *108*, 3384,
458 doi:10.1029/2002JC001347.
- 459 Comiso, J. C., C. L. Parkinson, R. Gersten, and L. Stock (2008), Accelerated decline in
460 the Arctic sea ice cover, *Geophys. Res. Lett.*, *35*, L01,703, doi:10.1029/2007GL031,972.
- 461 Connolley, W. M., J. M. Gregory, E. C. Hunke, and A. J. McLaren (2004), On the
462 consistent scaling of terms in the sea ice dynamics equation, *J. Phys. Oceanogr.*, *34*,
463 1776–1780.
- 464 Flato, G. M., and W. D. Hibler (1995), Ridging and strength in modeling the thickness
465 distribution of Arctic sea ice, *J. Geophys. Res.–Oceans*, *100*, 18,611–18,626.
- 466 Fowler, C., W. J. Emery, and J. Maslanik (2004), Satellite-derived evolution of Arctic sea
467 ice age: October 1978 to March 2003, *IEEE Geosci. Rem. Sens. Lett.*, *1*, 71–74.
- 468 Gillett, N. P., M. Allen, R. E. McDonald, C. A. Senior, D. T. Shindell, and G. A. Schmidt
469 (2002), How linear is the Arctic Oscillation response to greenhouse gases?, *J. Geophys.*
470 *Res.*, *107*, ACL 1–1–1–7, 0.1029/2001JD000,589.
- 471 Gloersen, P., W. J. Campbell, D. J. Cavalieri, J. C. Comiso, C. L. Parkinson, and H. J.
472 Zwally (1992), Arctic and Antarctic sea ice, 1978–1987: Satellite passive-microwave
473 observations and analysis, *Tech. Rep. SP-511*, NASA.



- 474 Hibler, W. D. (1980), Modeling a variable thickness sea ice cover, *Mon. Wea. Rev.*, *108*,
475 1943–1973.
- 476 Holland, M. M., and C. M. Bitz (2003), Polar amplification of climate change in coupled
477 models, *Climate Dyn.*, *21*, 221–232.
- 478 Hunke, E., and M. Holland (2007), Global atmospheric forcing data for Arctic ice-ocean
479 modeling, *J. Geophys. Res.*, *112*, C06S14, doi:10.1029/2006JC003,640.
- 480 Hunke, E. C., and J. K. Dukowicz (2002), The Elastic-Viscous-Plastic sea ice dynamics
481 model in general orthogonal curvilinear coordinates on a sphere—Effect of metric terms,
482 *Mon. Wea. Rev.*, *130*, 1848–1865.
- 483 Hunke, E. C., and W. H. Lipscomb (2008), CICE: the Los Alamos Sea Ice Model, Doc-
484 umentation and Software User’s Manual, version 4.0, *Tech. Rep. LA-CC-06-012*, Los
485 Alamos National Laboratory, Los Alamos, New Mexico.
- 486 Johannessen, O. M., E. V. Shalina, and M. W. Miles (1999), Satellite evidence for an
487 Arctic sea-ice cover in transformation, *Science*, *286*, 1937–1939.
- 488 Kiehl, J. T., and P. R. Gent (2004), The Community Climate System Model, Version
489 Two, *J. Climate*, *17*, 3666–3682.
- 490 Kwok, R., and D. A. Rothrock (1999), Variability of Fram Strait ice flux and North
491 Atlantic Oscillation, *J. Geophys. Res.*, *104*, 5177–5189.
- 492 Kwok, R., G. F. Cunningham, and S. S. Pang (2004a), Fram Strait sea ice outflow, *J.*
493 *Geophys. Res.*, *109*, C01,009, doi:10.1029/2003JC001,785.
- 494 Kwok, R., H. J. Zwally, and D. Yi (2004b), ICESat observations of Arctic Ocean sea ice:
495 A first look, *Geophys. Res. Lett.*, *31*, L16,401, doi:10.1029/2004GL020,309.



- 496 Large, W., and S. Yeager (2004), Diurnal to decadal global forcing for ocean and sea-ice
497 models: The data sets and flux climatologies, *NCAR Tech. Note NCAR/TN-460+STR*,
498 CGD Division of the National Center for Atmospheric Research.
- 499 Large, W., and S. Yeager (2008), The global climatology of an interannually varying
500 air-sea flux data set, *Clim. Dyn.*, Submitted.
- 501 Laxon, S., N. Peacock, and D. Smith (2003), High interannual variability of sea ice thick-
502 ness in the Arctic region, *Nature*, *425*, 947–950.
- 503 Lipscomb, W. H. (2001), Remapping the thickness distribution in sea ice models, *J.*
504 *Geophys. Res.–Oceans*, *106*, 13,989–14,000.
- 505 Lipscomb, W. H., and E. C. Hunke (2004), Modeling sea ice transport using incremental
506 remapping, *Mon. Wea. Rev.*, *132*, 1341–1354.
- 507 Lipscomb, W. H., E. C. Hunke, W. Maslowski, and J. Jakacki (2007), Improving ridging
508 schemes for high-resolution sea ice models, *J. Geophys. Res.–Oceans*, *112*, C03S91,
509 doi:10.1029/2005JC003,355.
- 510 Lizotte, M. P. (2001), The contributions of sea ice algae to Antarctic marine primary
511 production, *Amer. Zoologist*, *41*, 57–73.
- 512 Maslanik, J. A., C. Fowler, J. Stroeve, S. Drobot, J. Zwally, D. Yi, and W. Emery (2007),
513 A younger, thinner Arctic ice cover: Increased potential for rapid, extensive sea-ice loss,
514 *Geophys. Res. Lett.*, *34*, L24,501, doi:10.1029/2007GL032,043.
- 515 Nghiem, S. V., I. G. Rigor, D. K. Perovich, P. Clemente-Colon, J. W. Weatherly, and
516 G. Neumann (2007), Rapid reduction of Arctic perennial ice, *Geophys. Res. Lett.*, *34*,
517 L19,504, doi:10.1029/2007GL031,138.



- 518 Perovich, D. K. (2003), Complex yet translucent: the optical properties of sea ice, *Phys.*
519 *B*, *338*, 107–114.
- 520 Perovich, D. K., J. A. Richter-Menge, K. F. Jones, and B. Light (2008), Sunlight, water,
521 and ice: Extreme Arctic sea ice melt during the summer of 2007, *Geophys. Res. Lett.*,
522 *35*, L11,501, doi:10.1029/2008GL034,007.
- 523 Rigor, I. G., and J. M. Wallace (2004), Variations in the age of Arctic sea-ice and summer
524 sea-ice extent, *Geophys. Res. Lett.*, *31*, 109401, doi:10.1029/2004GL019492.
- 525 Rigor, I. G., J. M. Wallace, and R. L. Colony (2002), Response of sea ice to the Arctic
526 Oscillation, *J. Climate*, *15*, 2648–2663.
- 527 Röske, F. (2001), An atlas of surface fluxes based on the ECMWF reanalysis—A cli-
528 matological dataset to force global ocean general circulation models, *Tech. Rep. 323*,
529 Max-Planck-Institut für Meteorologie.
- 530 Rothrock, D. A. (1975), The energetics of the plastic deformation of pack ice by ridging,
531 *J. Geophys. Res.*, *80*, 4514–4519.
- 532 Rothrock, D. A., Y. Yu, and G. A. Maykut (1999), Thinning of the Arctic sea-ice cover,
533 *Geophys. Res. Lett.*, *26*, 3469–3472.
- 534 Smith, D. M. (1998), Recent increase in the length of the melt season of perennial Arctic
535 sea ice, *Geophys. Res. Lett.*, *25*, 655–658.
- 536 Thorndike, A. S., D. A. Rothrock, G. A. Maykut, and R. Colony (1975), The thickness
537 distribution of sea ice, *J. Geophys. Res.*, *80*, 4501–4513.
- 538 Wadhams, P. (1990), Evidence for thinning of the Arctic ice cover north of Greenland,
539 *Nature*, *345*, 795–797.



- 540 Wadhams, P., and N. R. Davis (2000), Further evidence of ice thinning in the Arctic
541 Ocean, *Geophys. Res. Lett.*, *27*, 3973–3975.
- 542 WMO (1989), *Sea-Ice Nomenclature, No. 259 Suppl. No. 5*, World Meteorological Orga-
543 nization, Geneva, Switzerland.
- 544 Zhang, X., and J. E. Walsh (2006), Toward a seasonally ice-covered Arctic Ocean: Sce-
545 narios from the IPCC AR4 model simulations, *J. Clim.*, *19*, 1730–1747.



546 **Figure Captions**

547

548 Figure 1. (a) Volume and area of all Arctic ice, (b) volume, area and average thickness of
 549 perennial ice, (c) area of seasonal ice, (d) September seasonal ice area and total ice area anomaly
 550 from the 1977–2006 mean, and (e) area-weighted average age of perennial ice and the whole
 551 Arctic ice pack. The legend for panels (a)–(c) is in panel (b).

552 Figure 2. Winter (Nov.–Apr.) area flux through Fram Strait. Satellite-based observational
 553 data [*Kwok et al.*, 2004a] is dashed.

554 Figure 3. Monthly climatologies of perennial ice volume, area, thickness and area-weighted
 555 average age for the three decades shown in the lower panel.

556 Figure 4. Average March thickness of ice plotted against ice age, for three decades, and the
 557 *Maslanik et al.* [2007] proxy ice thickness estimates for 2003–2006. Model data are plotted only
 558 for age bins that are populated for all 10 years of each averaging period.

559 Figure 5. March ice thickness, in m, for (a) 1976, (b) 1986 (c) 1996, (d) 2006, overlain with
 560 ice age contours in black (2-year increments). The 15% area concentration contour is white.

561 Figure 6. (a) For September of each year, the total area of ice of age N indicated on the x-axis.
 562 For March of each year, (b) the total area of ice of age greater or equal to N , (c) the age of ice
 563 passing through Fram Strait (years). A 4-year running mean has been applied in (a) to smooth
 564 the seasonal cycle.

565 Figure 7. Area-weighted average age of perennial ice and the whole Arctic ice pack (a) in the
 566 control run, in which accretion at the bottom of the ice did not influence ice age, and (b) in the
 567 sensitivity run, in which bottom growth was included in the ice age.



	March		September	
	mean	trend	mean	trend
seasonal area	8.0	0.29	0.3	-0.01
perennial area	7.0	-0.42	5.5	-0.61
total ice area	15.0	-0.13	5.8	-0.62
average age	2.9	-0.27	6.5	-0.13

Table 1. Mean March and September 1977–2006 seasonal, perennial and total ice area (10^6 km²), area-weighted average age (years), and their trends per decade, for the Northern Hemisphere.

	<i>Smith</i> [1998]		<i>Belchansky et al.</i> [2004]		CICE	
	mean	trend	mean	trend	mean	trend
melt onset	164	-0.7	169	-4.0	141	-4.9
freeze onset	240	+3.7	238	+1.4	233	+1.8
melt season	75	+4.5	68	+5.5	91	+6.7

Table 2. Mean 1979–1996 melt and freeze onset dates (Julian day) and melt season length (days) for perennial ice, and their trends (days per decade).



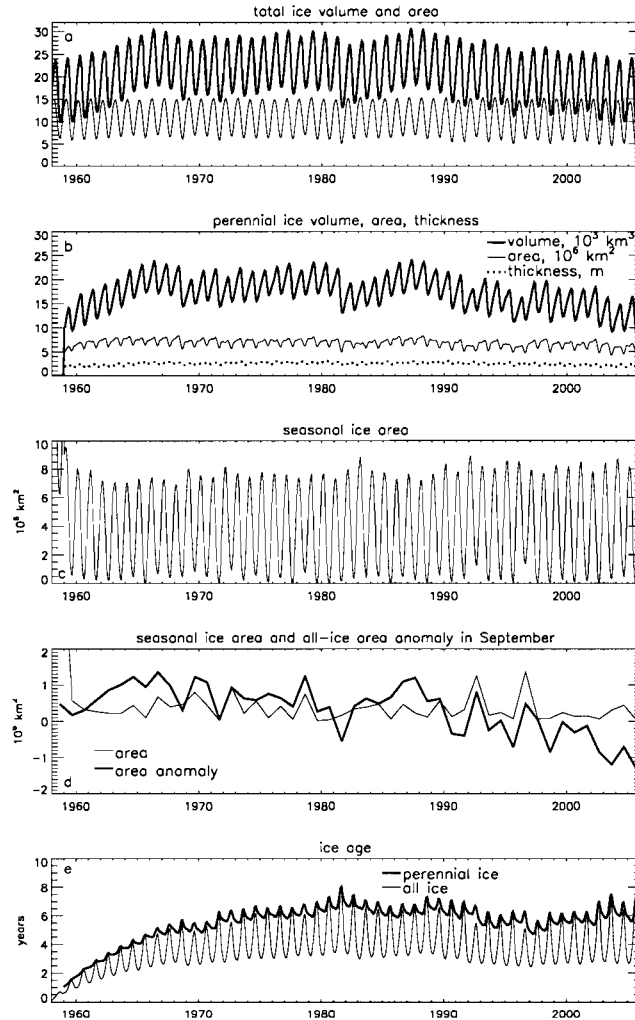


Figure 1. (a) Volume and area of all Arctic ice, (b) volume, area and average thickness of perennial ice, (c) area of seasonal ice, (d) September seasonal ice area and total ice area anomaly from the 1977–2006 mean, and (e) area-weighted average age of perennial ice and the whole Arctic ice pack. The legend for panels (a)–(c) is in panel (b).



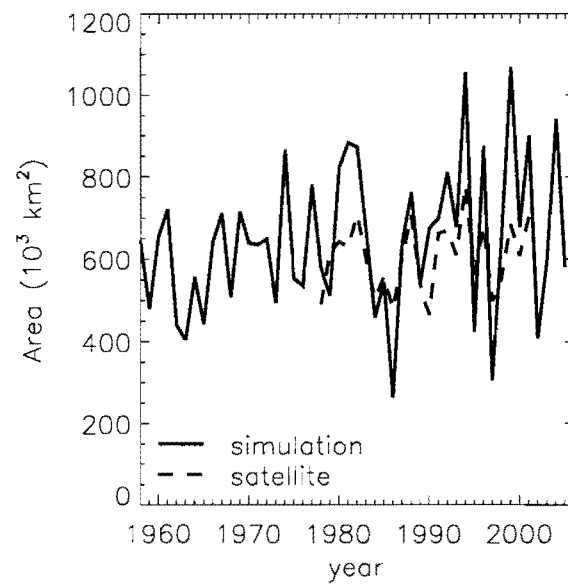


Figure 2. Winter (Nov.–Apr.) area flux through Fram Strait. Satellite-based observational data [Kwok *et al.*, 2004a] is dashed.



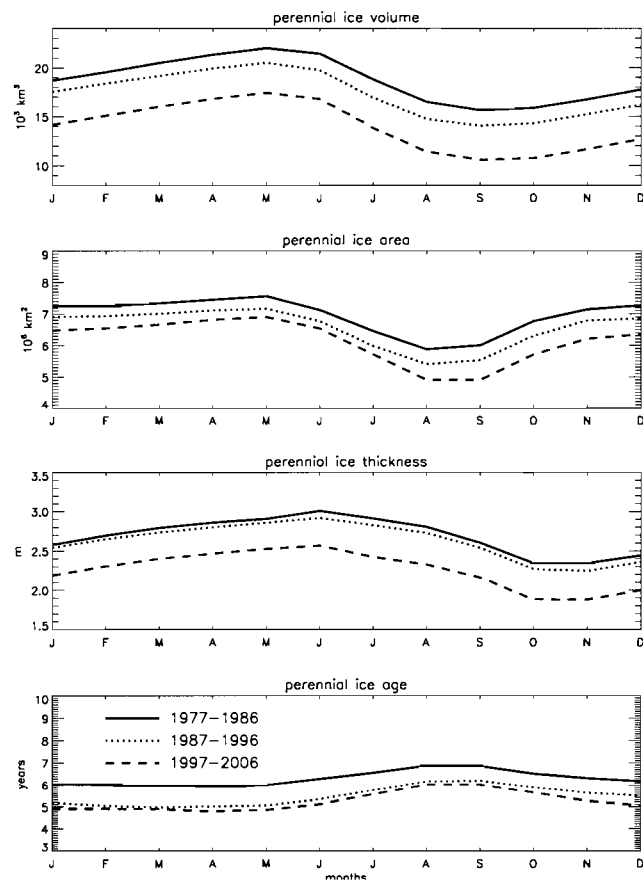


Figure 3. Monthly climatologies of perennial ice volume, area, thickness and area-weighted average age for the three decades shown in the lower panel.



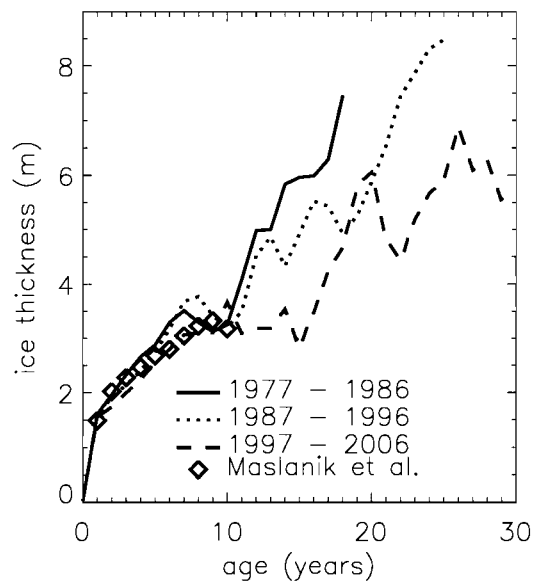


Figure 4. Average March thickness of ice plotted against ice age, for three decades, and the *Maslanik et al.* [2007] proxy ice thickness estimates for 2003–2006. Model data are plotted only for age bins that are populated for all 10 years of each averaging period.



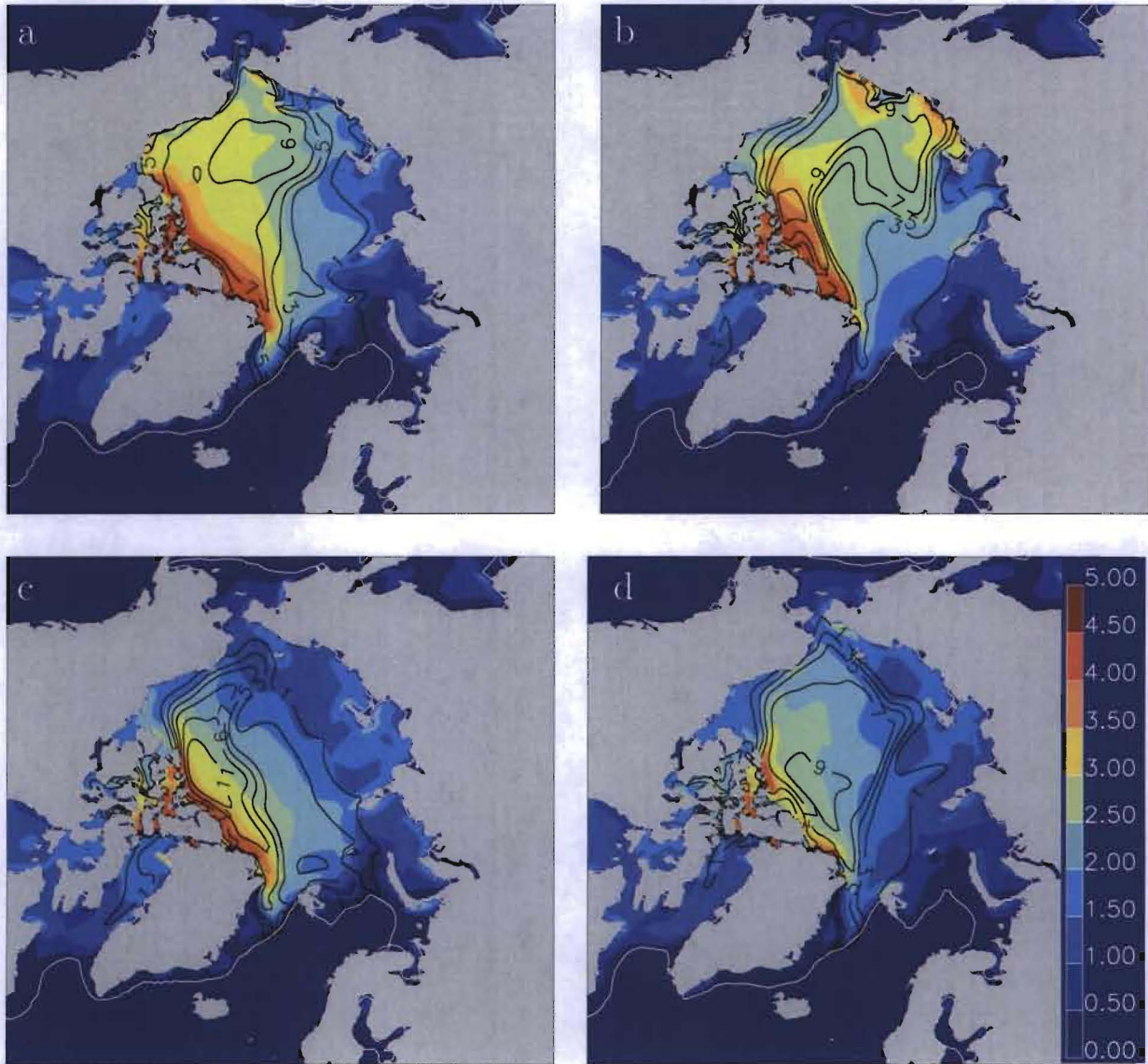


Figure 5. March ice thickness, in m, for (a) 1976, (b) 1986 (c) 1996, (d) 2006, overlain with ice age contours in black (2-year increments). The 15% area concentration contour is white.



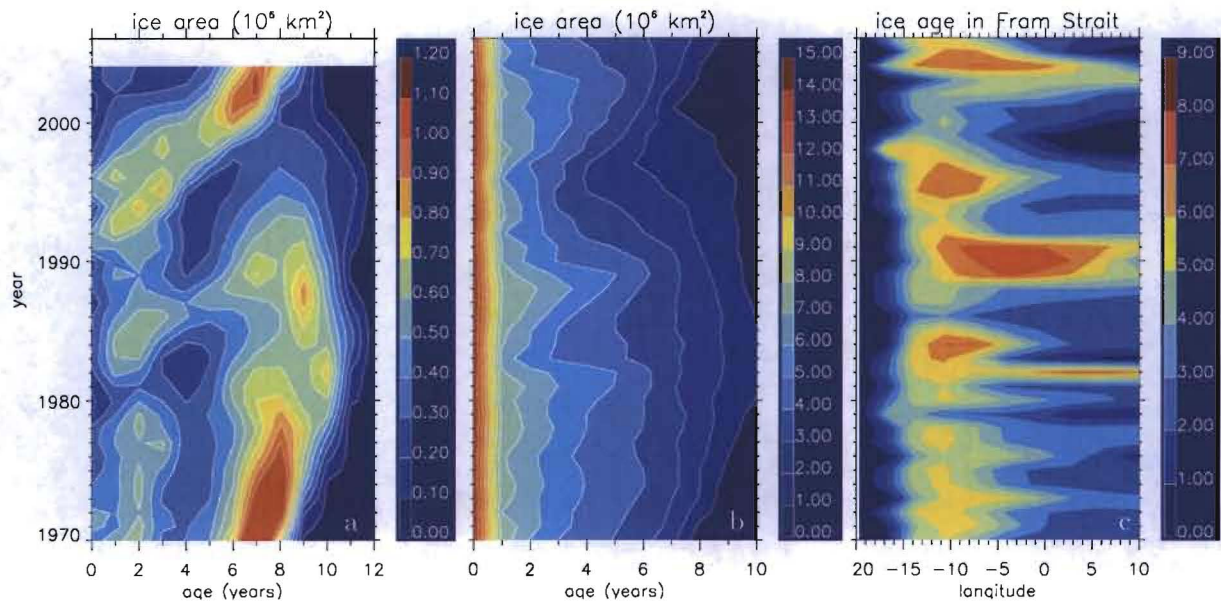


Figure 6. (a) For September of each year, the total area of ice of age N indicated on the x-axis. For March of each year, (b) the total area of ice of age greater or equal to N , (c) the age of ice passing through Fram Strait (years). A 4-year running mean has been applied in (a) to smooth the seasonal cycle.



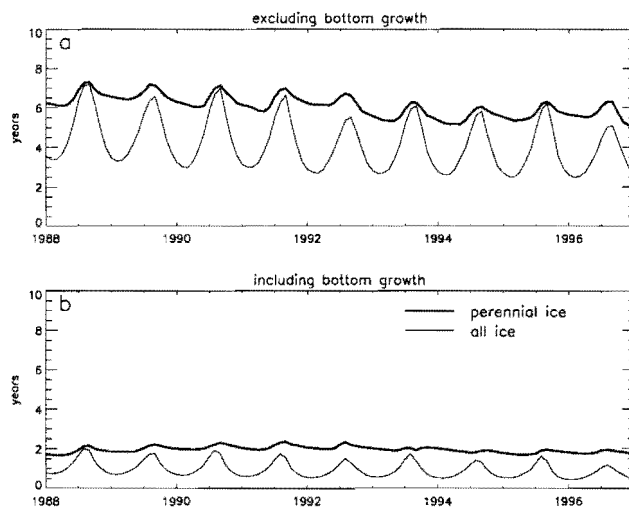


Figure 7. Area-weighted average age of perennial ice and the whole Arctic ice pack (a) in the control run, in which accretion at the bottom of the ice did not influence ice age, and (b) in the sensitivity run, in which bottom growth was included in the ice age.

